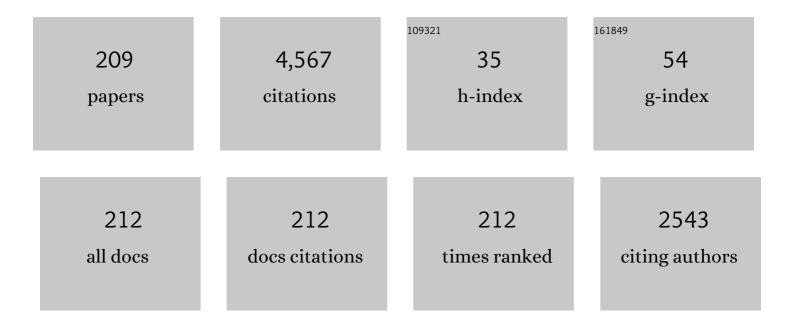
Dimitrios Maroudas

List of Publications by Year in descending order

Source: https://exaly.com/author-pdf/2058794/publications.pdf Version: 2024-02-01



#	Article	IF	CITATIONS
1	Effect of helium flux on near-surface helium accumulation in plasma-exposed tungsten. Journal of Physics Condensed Matter, 2022, 34, 035701.	1.8	2
2	Hole formation effect on surface morphological response of plasma-facing tungsten. Journal of Applied Physics, 2021, 129, 193302.	2.5	6
3	Strain Effects on the Diffusion Properties of Near-Surface Self-Interstitial Atoms and Adatoms in Tungsten. Frontiers in Materials, 2021, 8, .	2.4	1
4	Molecular-Dynamics Simulations on Nanoindentation of Graphene-Diamond Composite Superstructures in Interlayer-Bonded Twisted Bilayer Graphene: Implications for Mechanical Metamaterials. ACS Applied Nano Materials, 2021, 4, 8611-8625.	5.0	9
5	Effects of elastic softening and helium accumulation kinetics on surface morphological evolution of plasma-facing tungsten. Nuclear Fusion, 2021, 61, 016016.	3.5	11
6	Onset of fuzz formation in plasma-facing tungsten as a surface morphological instability. Physical Review Materials, 2021, 5, .	2.4	6
7	Thermal gradient effect on helium and self-interstitial transport in tungsten. Journal of Applied Physics, 2021, 130, .	2.5	2
8	Fabrication of Ordered Arrays of Quantum Dot Molecules Based on the Design of Pyramidal Pit Patterns on Semiconductor Surfaces. Industrial & Engineering Chemistry Research, 2020, 59, 2536-2547.	3.7	3
9	Non-dilute helium-related defect interactions in the near-surface region of plasma-exposed tungsten. Journal of Applied Physics, 2020, 128, .	2.5	6
10	Prediction of temperature range for the onset of fuzz formation in helium-plasma-implanted tungsten. Surface Science, 2020, 698, 121614.	1.9	17
11	Theoretical Model of Helium Bubble Growth and Density in Plasma-Facing Metals. Scientific Reports, 2020, 10, 2192.	3.3	34
12	Molecular-Dynamics Analysis of Nanoindentation of Graphene Nanomeshes: Implications for 2D Mechanical Metamaterials. ACS Applied Nano Materials, 2020, 3, 3613-3624.	5.0	6
13	Elastic Properties of Plasma-Exposed Tungsten Predicted by Molecular-Dynamics Simulations. ACS Applied Materials & Interfaces, 2020, 12, 22287-22297.	8.0	20
14	On the origin of â€~fuzz' formation in plasma-facing materials. Nuclear Fusion, 2019, 59, 086057.	3.5	56
15	Theoretical design of new cyclopentadithiophene-based organic semiconductors with tunable nature and performance. Synthetic Metals, 2019, 258, 116196.	3.9	4
16	On the formation of multiple quantum dots inside elongated pits on semiconductor films deposited epitaxially on pit-patterned substrates. Materials Research Express, 2019, 6, 086328.	1.6	3
17	Design of semiconductor surface pits for fabrication of regular arrays of quantum dots and nanorings. Journal of Applied Physics, 2019, 125, .	2.5	4
18	Structure-properties relations in graphene derivatives and metamaterials obtained by atomic-scale modeling. Molecular Simulation, 2019, 45, 1173-1202.	2.0	6

#	Article	IF	CITATIONS
19	Atomic-scale modeling toward enabling models of surface nanostructure formation in plasma-facing materials. Current Opinion in Chemical Engineering, 2019, 23, 77-84.	7.8	3
20	Helium flux effects on bubble growth and surface morphology in plasma-facing tungsten from large-scale molecular dynamics simulations. Nuclear Fusion, 2019, 59, 066035.	3.5	37
21	Effects of pore morphology and pore edge termination on the mechanical behavior of graphene nanomeshes. Journal of Applied Physics, 2019, 126, 164306.	2.5	9
22	Large-scale atomistic simulations of low-energy helium implantation into tungsten single crystals. Acta Materialia, 2018, 144, 561-578.	7.9	89
23	Analysis of current-driven oscillatory dynamics of single-layer homoepitaxial islands on crystalline conducting substrates. Surface Science, 2018, 669, 25-33.	1.9	12
24	Optimization of electrical treatment strategy for surface roughness reduction in conducting thin films. Journal of Applied Physics, 2018, 124, 125302.	2.5	8
25	Electronic structure of electron-irradiated graphene and effects of hydrogen passivation. Materials Research Express, 2018, 5, 115603.	1.6	9
26	Modeling of quantum dot and nanoring pattern formation on pit-patterned semiconductor substrates. Materials Research Express, 2018, 5, 086303.	1.6	3
27	Formation and Mechanical Behavior of Nanocomposite Superstructures from Interlayer Bonding in Twisted Bilayer Graphene. ACS Applied Materials & Interfaces, 2018, 10, 28898-28908.	8.0	33
28	Helium segregation and transport behavior near ⟠100⟩ and ⟠110⟩ symmetric tilt grain boundaries in tungsten. Journal of Applied Physics, 2018, 123, .	2.5	22
29	Kinetics of nanoring formation on surfaces of stressed thin films. Physical Review Materials, 2018, 2, .	2.4	4
30	Current-induced surface roughness reduction in conducting thin films. Applied Physics Letters, 2017, 110, 103103.	3.3	8
31	Multiscale Shear-Lag Analysis of Stiffness Enhancement in Polymer–Graphene Nanocomposites. ACS Applied Materials & Interfaces, 2017, 9, 23092-23098.	8.0	19
32	Dynamics of Small Mobile Helium Clusters Near a Symmetric Tilt Grain Boundary of Plasma-Exposed Tungsten. Fusion Science and Technology, 2017, 71, 36-51.	1.1	16
33	Complex Pattern Formation from Current-Driven Dynamics of Single-Layer Homoepitaxial Islands on Crystalline Conducting Substrates. Physical Review Applied, 2017, 8, .	3.8	9
34	Thermal conductivity of electron-irradiated graphene. Applied Physics Letters, 2017, 111, .	3.3	9
35	Thermal conductivity of tungsten: Effects of plasma-related structural defects from molecular-dynamics simulations. Applied Physics Letters, 2017, 111, .	3.3	35
36	Benchmarks and Tests of a Multidimensional Cluster Dynamics Model of Helium Implantation in Tungsten. Fusion Science and Technology, 2017, 71, 84-92.	1.1	20

#	Article	IF	CITATIONS
37	Modeling Helium Segregation to the Surfaces of Plasma-Exposed Tungsten as a Function of Temperature and Surface Orientation. Fusion Science and Technology, 2017, 71, 22-35.	1.1	18
38	Charge transfer properties of diphenyl substituted cyclopentadithiophene organic semiconductors: The role of fluorine and malononitrile substitutions and crystal ordering. Organic Electronics, 2017, 50, 130-137.	2.6	9
39	Tuning the band structure of graphene nanoribbons through defect-interaction-driven edge patterning. Physical Review B, 2017, 96, .	3.2	6
40	Current-driven nanowire formation on surfaces of crystalline conducting substrates. Applied Physics Letters, 2016, 108, 193109.	3.3	15
41	Theory of multiple quantum dot formation in strained-layer heteroepitaxy. Applied Physics Letters, 2016, 109, .	3.3	19
42	Mechanical properties of hydrogenated electron-irradiated graphene. Journal of Applied Physics, 2016, 120, 124301.	2.5	11
43	Surface nanopattern formation due to current-induced homoepitaxial nanowire edge instability. Applied Physics Letters, 2016, 109, .	3.3	6
44	Helium segregation on surfaces of plasma-exposed tungsten. Journal of Physics Condensed Matter, 2016, 28, 064004.	1.8	40
45	A Comparison of the Elastic Properties of Graphene- and Fullerene-Reinforced Polymer Composites: The Role of Filler Morphology and Size. Scientific Reports, 2016, 6, 31735.	3.3	46
46	Evidence for reduced charge recombination in carbon nanotube/perovskite-based active layers. Chemical Physics Letters, 2016, 662, 35-41.	2.6	43
47	Tunable Percolation in Semiconducting Binary Polymer Nanoparticle Glasses. Journal of Physical Chemistry B, 2016, 120, 2544-2556.	2.6	3
48	Molecular-dynamics analysis of mobile helium cluster reactions near surfaces of plasma-exposed tungsten. Journal of Applied Physics, 2015, 118, .	2.5	47
49	Weakly nonlinear theory of secondary rippling instability in surfaces of stressed solids. Journal of Applied Physics, 2015, 118, .	2.5	10
50	Equilibrium Shape of Colloidal Crystals. Langmuir, 2015, 31, 11428-11437.	3.5	9
51	Analysis of Charge Transport and Device Performance in Organic Photovoltaic Devices with Active Layers of Self-Assembled Nanospheres. Journal of Physical Chemistry C, 2015, 119, 25826-25839.	3.1	15
52	Mechanical behavior and fracture of graphene nanomeshes. Journal of Applied Physics, 2015, 117, .	2.5	28
53	Controlling assembly of colloidal particles into structured objects: Basic strategy and a case study. Journal of Process Control, 2015, 27, 64-75.	3.3	33
54	Helium impurity transport on grain boundaries: Enhanced or inhibited?. Europhysics Letters, 2015, 110, 52002.	2.0	38

#	Article	IF	CITATIONS
55	Mechanical behavior of interlayer-bonded nanostructures obtained from bilayer graphene. Carbon, 2015, 81, 663-677.	10.3	64
56	Interactions of mobile helium clusters with surfaces and grain boundaries of plasma-exposed tungsten. Journal of Applied Physics, 2014, 115, .	2.5	66
57	Stabilization of the surface morphology of stressed solids using thermal gradients. Applied Physics Letters, 2014, 104, .	3.3	9
58	Thermal transport properties of graphene nanomeshes. Journal of Applied Physics, 2014, 116, 184304.	2.5	23
59	Phase behavior of the 38-atom Lennard-Jones cluster. Journal of Chemical Physics, 2014, 140, 104312.	3.0	11
60	Dynamics of small mobile helium clusters near tungsten surfaces. Surface Science, 2014, 626, L21-L25.	1.9	73
61	Elastic properties of graphene nanomeshes. Applied Physics Letters, 2014, 104, .	3.3	42
62	Stabilization of the surface morphology of stressed solids using simultaneously applied electric fields and thermal gradients. Journal of Applied Physics, 2014, 116, .	2.5	5
63	Effects of the Attractive Potential Range on the Phase Behavior of Small Clusters of Colloidal Particles. Journal of Chemical & Engineering Data, 2014, 59, 3105-3112.	1.9	0
64	Design of semiconductor ternary quantum dots with optimal optoelectronic function. AICHE Journal, 2013, 59, 3223-3236.	3.6	9
65	Superlattices of Fluorinated Interlayer-Bonded Domains in Twisted Bilayer Graphene. Journal of Physical Chemistry C, 2013, 117, 7315-7325.	3.1	41
66	Onset of the crystalline phase in small assemblies of colloidal particles. Applied Physics Letters, 2013, 102, .	3.3	7
67	Current-driven morphological evolution of single-layer epitaxial islands on crystalline substrates. Surface Science, 2013, 618, L1-L5.	1.9	13
68	The effect of a thermal gradient on the electromigration-driven surface morphological stabilization of an epitaxial thin film on a compliant substrate. Journal of Applied Physics, 2013, 114, 023503.	2.5	4
69	Mechanical properties of irradiated single-layer graphene. Applied Physics Letters, 2013, 103, 013102.	3.3	59
70	Surface nanopatterning from current-driven assembly of single-layer epitaxial islands. Applied Physics Letters, 2013, 103, .	3.3	14
71	Tunable mechanical properties of diamond superlattices generated by interlayer bonding in twisted bilayer graphene. Applied Physics Letters, 2013, 103, .	3.3	38
72	Analysis of vacancy-induced amorphization of single-layer graphene. Applied Physics Letters, 2012, 100, 203105.	3.3	22

#	Article	IF	CITATIONS
73	The effect of a compliant substrate on the electromigration-driven surface morphological stabilization of an epitaxial thin film. Journal of Applied Physics, 2012, 111, 024905.	2.5	5
74	Surface morphological stabilization of stressed crystalline solids by simultaneous action of applied electric and thermal fields. Applied Physics Letters, 2012, 100, .	3.3	10
75	Electromigration-driven complex dynamics of void surfaces in stressed metallic thin films under a general biaxial mechanical loading. Journal of Applied Physics, 2012, 112, 083523.	2.5	1
76	Kinetics of interdiffusion in semiconductor ternary quantum dots. Applied Physics Letters, 2012, 101, .	3.3	3
77	Colloidal cluster crystallization dynamics. Journal of Chemical Physics, 2012, 137, 134901.	3.0	22
78	Opening and tuning of band gap by the formation of diamond superlattices in twisted bilayer graphene. Physical Review B, 2012, 86, .	3.2	68
79	Thermodynamic instability of ZnSe/ZnS core/shell quantum dots. Journal of Applied Physics, 2012, 111, 113526.	2.5	9
80	Formation of fullerene superlattices by interlayer bonding in twisted bilayer graphene. Journal of Applied Physics, 2012, 111, .	2.5	35
81	Surface morphological response of crystalline solids to mechanical stresses and electric fields. Surface Science Reports, 2011, 66, 299-346.	7.2	31
82	Effect of applied stress tensor anisotropy on the electromechanically driven complex dynamics of void surfaces in metallic thin films. Journal of Applied Physics, 2011, 110, .	2.5	1
83	Equilibrium compositional distribution in freestanding ternary semiconductor quantum dots: The case of InxGa1â^'xAs. Journal of Chemical Physics, 2011, 135, 234701.	3.0	5
84	Mechanical properties of ultralow-dielectric-constant mesoporous amorphous silica structures: Effects of pore morphology and loading mode. Applied Physics Letters, 2011, 98, .	3.3	4
85	Compositional effects on the electronic structure of ZnSe1â^'xSx ternary quantum dots. Applied Physics Letters, 2011, 99, .	3.3	5
86	Effects of composition and compositional distribution on the electronic structure of ZnSe1â^'xTex ternary quantum dots. Journal of Applied Physics, 2011, 110, 123509.	2.5	3
87	Theory of surface segregation in ternary semiconductor quantum dots. Applied Physics Letters, 2011, 98, .	3.3	13
88	Analysis of electromechanically induced long-wavelength rippling instability on surfaces of crystalline conductors. Journal of Applied Physics, 2011, 109, 053518.	2.5	7
89	A Smoluchowski model of crystallization dynamics of small colloidal clusters. Journal of Chemical Physics, 2011, 135, 154506.	3.0	23
90	Electromigration-driven surface morphological stabilization of a coherently strained epitaxial thin film on a substrate. Applied Physics Letters, 2010, 96, 231911.	3.3	13

#	Article	IF	CITATIONS
91	Current-induced stabilization of surface morphology in stressed solids: Validation of linear stability theory. Journal of Applied Physics, 2010, 107, .	2.5	13
92	Formation of core/shell-like ZnSe1â^'xTex nanocrystals due to equilibrium surface segregation. Applied Physics Letters, 2010, 96, .	3.3	7
93	Electromechanically driven chaotic dynamics of voids in metallic thin films. Physical Review B, 2010, 81, .	3.2	4
94	Analysis of current-driven surface morphological stabilization of a coherently strained epitaxial thin film on a finite-thickness deformable substrate. Journal of Applied Physics, 2010, 108, 093517.	2.5	10
95	Effects of surface diffusional anisotropy on the current-driven surface morphological response of stressed solids. Journal of Applied Physics, 2010, 107, 093527.	2.5	14
96	Analysis of current-driven motion of morphologically stable voids in metallic thin films: Steady and time-periodic states. Journal of Applied Physics, 2010, 108, 053514.	2.5	4
97	Hydrogenation effects on the structure and morphology of graphene and single-walled carbon nanotubes. Journal of Applied Physics, 2010, 108, 113532.	2.5	12
98	Comparative study of the mechanical behavior under biaxial strain of prestrained face-centered cubic metallic ultrathin films. Applied Physics Letters, 2009, 94, 101911.	3.3	12
99	On the hydrogen storage capacity of carbon nanotube bundles. Applied Physics Letters, 2009, 95, 163111.	3.3	21
100	Rippling instability on surfaces of stressed crystalline conductors. Applied Physics Letters, 2009, 94, 181911.	3.3	14
101	Analysis of diamond nanocrystal formation from multiwalled carbon nanotubes. Physical Review B, 2009, 80, .	3.2	18
102	Dynamics of the <mml:math <br="" xmlns:mml="http://www.w3.org/1998/Math/MathML">display="inline"><mml:mrow><mml:mtext>bcc</mml:mtext><mml:mo>→</mml:mo><mml:mtext>hcpin crystals under uniaxial stress. Physical Review B, 2009, 79, .</mml:mtext></mml:mrow></mml:math>	nte st 2 <td>ml:114row></td>	ml :11 4row>
103	Molecular-dynamics simulations of stacking-fault-induced dislocation annihilation in prestrained ultrathin single-crystalline copper films. Journal of Applied Physics, 2009, 105, .	2.5	26
104	Atomistic analysis of strain relaxation in [11Â ⁻ 0]-oriented biaxially strained ultrathin copper films. Journal of Applied Physics, 2009, 106, 103519.	2.5	2
105	First-principles theoretical analysis of pure and hydrogenated crystalline carbon phases and nanostructures. Chemical Physics Letters, 2009, 474, 168-174.	2.6	11
106	Effects of hydrogen chemisorption on the structure and deformation of single-walled carbon nanotubes. Applied Physics Letters, 2009, 94, .	3.3	25
107	Kinetic Monte Carlo simulations of surface growth during plasma deposition of silicon thin films. Journal of Chemical Physics, 2009, 131, 034503.	3.0	18
108	Hopf bifurcation, bistability, and onset of current-induced surface wave propagation on void surfaces in metallic thin films. Surface Science, 2008, 602, 1227-1242.	1.9	15

#	Article	IF	CITATIONS
109	First-principles theoretical analysis of dopant adsorption and diffusion on surfaces of ZnSe nanocrystals. Chemical Physics Letters, 2008, 462, 265-268.	2.6	3
110	Atomic-scale analysis of defect dynamics and strain relaxation mechanisms in biaxially strained ultrathin films of face-centered cubic metals. Journal of Applied Physics, 2008, 103, .	2.5	21
111	Coarse molecular-dynamics analysis of an order-to-disorder transformation of a krypton monolayer on graphite. Journal of Chemical Physics, 2008, 129, 184106.	3.0	5
112	Mechanical behavior of ultralow-dielectric-constant mesoporous amorphous silica. Applied Physics Letters, 2008, 92, 251903.	3.3	5
113	On the growth mechanism of plasma deposited amorphous silicon thin films. Applied Physics Letters, 2008, 93, 151913.	3.3	4
114	Current-Induced Stabilization of Surface Morphology in Stressed Solids. Physical Review Letters, 2008, 100, 036106.	7.8	42
115	Molecular dynamics simulations of martensitic fcc-to-hcp phase transformations in strained ultrathin metallic films. Physical Review B, 2008, 78, .	3.2	19
116	Theoretical analysis of texture effects on the surface morphological stability of metallic thin films. Applied Physics Letters, 2008, 92, 181905.	3.3	19
117	Interactions between radical growth precursors on plasma-deposited silicon thin-film surfaces. Journal of Chemical Physics, 2007, 126, 114704.	3.0	10
118	Current-induced wave propagation on surfaces of voids in metallic thin films with high symmetry of surface diffusional anisotropy. Journal of Applied Physics, 2007, 102, 073506.	2.5	6
119	Stability of simple cubic crystals. Applied Physics Letters, 2007, 90, 161910.	3.3	11
120	Stress-induced deceleration of electromigration-driven void motion in metallic thin films. Journal of Applied Physics, 2007, 101, 063513.	2.5	16
121	Theoretical analysis of current-driven interactions between voids in metallic thin films. Journal of Applied Physics, 2007, 101, 023518.	2.5	13
122	First-principles theoretical analysis of sequential hydride dissociation on surfaces of silicon thin films. Applied Physics Letters, 2007, 90, 251915.	3.3	7
123	Void nucleation in biaxially strained ultrathin films of face-centered cubic metals. Applied Physics Letters, 2007, 90, 221907.	3.3	12
124	Coarse molecular-dynamics analysis of stress-induced structural transitions in crystals. Applied Physics Letters, 2007, 90, 171910.	3.3	8
125	Mechanisms and energetics of hydride dissociation reactions on surfaces of plasma-deposited silicon thin films. Journal of Chemical Physics, 2007, 127, 194703.	3.0	7
126	Hydrogen-induced crystallization of amorphous Si thin films. II. Mechanisms and energetics of hydrogen insertion into Si–Si bonds. Journal of Applied Physics, 2006, 100, 053515.	2.5	29

#	Article	IF	CITATIONS
127	Hydrogen-induced crystallization of amorphous silicon thin films. I. Simulation and analysis of film postgrowth treatment with H2 plasmas. Journal of Applied Physics, 2006, 100, 053514.	2.5	38
128	First-principles theoretical analysis of silyl radical diffusion on silicon surfaces. Journal of Chemical Physics, 2006, 125, 104702.	3.0	20
129	Surface smoothness of plasma-deposited amorphous silicon thin films: Surface diffusion of radical precursors and mechanism of Si incorporation. Physical Review B, 2006, 74, .	3.2	11
130	Current-driven interactions between voids in metallic interconnect lines and their effects on line electrical resistance. Applied Physics Letters, 2006, 88, 221905.	3.3	21
131	Coarse molecular-dynamics determination of the onset of structural transitions: Melting of crystalline solids. Physical Review B, 2006, 74, .	3.2	7
132	Analysis of elastic stability and structural response of face-centered cubic crystals subject to [110] loading. Applied Physics Letters, 2006, 89, 181907.	3.3	5
133	Atomic-scale analysis of fundamental mechanisms of surface valley filling during plasma deposition of amorphous silicon thin films. Surface Science, 2005, 574, 123-143.	1.9	11
134	Electromigration-induced wave propagation on surfaces of voids in metallic thin films: Hopf bifurcation for high grain symmetry. Surface Science, 2005, 575, L41-L50.	1.9	17
135	Interaction of SiH3 radicals with deuterated (hydrogenated) amorphous silicon surfaces. Surface Science, 2005, 598, 35-44.	1.9	20
136	Temperature dependence of precursor–surface interactions in plasma deposition of silicon thin films. Chemical Physics Letters, 2005, 414, 61-65.	2.6	16
137	Analysis of Electromigration- and Stress-Induced Dynamical Response of Voids Confined in Metallic Thin Films. Materials Research Society Symposia Proceedings, 2005, 899, 1.	0.1	0
138	Relaxation of biaxial tensile strain in ultrathin metallic films: Ductile void growth versus nanocrystalline domain formation. Applied Physics Letters, 2005, 87, 171913.	3.3	13
139	Atomistic analysis of the mechanism of hydrogen diffusion in plasma-deposited amorphous silicon thin films. Applied Physics Letters, 2005, 87, 261911.	3.3	10
140	Atomistic mechanisms of strain relaxation due to ductile void growth in ultrathin films of face-centered-cubic metals. Journal of Applied Physics, 2005, 97, 113527.	2.5	18
141	Thermally activated mechanisms of hydrogen abstraction by growth precursors during plasma deposition of silicon thin films. Journal of Chemical Physics, 2005, 122, 054703.	3.0	32
142	Surface Smoothening Mechanism of Amorphous Silicon Thin Films. Physical Review Letters, 2005, 95, 216102.	7.8	24
143	Applicability of Born's stability criterion to face-centered-cubic crystals in [111] loading. Applied Physics Letters, 2005, 87, 251919.	3.3	14
144	Effects of electromigration-induced void dynamics on the evolution of electrical resistance in metallic interconnect lines. Applied Physics Letters, 2005, 86, 241905.	3.3	18

#	Article	IF	CITATIONS
145	Atomic-Scale Analysis of Strain Relaxation Mechanisms in Ultra-Thin Metallic Films. Materials Research Society Symposia Proceedings, 2005, 880, 1.	0.1	0
146	The Role of SiH3 Diffusion in Determining the Surface Smoothness of Plasma-Deposited Amorphous Si Thin Films: An Atomic-Scale Analysis. Materials Research Society Symposia Proceedings, 2005, 862, 321.	0.1	0
147	Analysis of Electromigration-Induced Void Motion and Surface Oscillations in Metallic Thin-Film Interconnects. Materials Research Society Symposia Proceedings, 2005, 863, B9.8-1.	0.1	0
148	Strain Relaxation in Si1-xGex Thin Films on Si (100) Substrates: Modeling and Comparisons with Experiments. Materials Research Society Symposia Proceedings, 2005, 875, 1.	0.1	6
149	Hydrogen in Si–Si bond center and platelet-like defect configurations in amorphous hydrogenated silicon. Journal of Vacuum Science & Technology an Official Journal of the American Vacuum Society B, Microelectronics Processing and Phenomena, 2004, 22, 2719.	1.6	20
150	Atomic pattern formation at the onset of stress-induced elastic instability: Fracture versus phase change. Physical Review B, 2004, 70, .	3.2	19
151	Electromigration-driven motion of morphologically stable voids in metallic thin films: Universal scaling of migration speed with void size. Applied Physics Letters, 2004, 85, 2214-2216.	3.3	32
152	Surface Processes during Growth of Hydrogenated Amorphous Silicon. Materials Research Society Symposia Proceedings, 2004, 808, 311.	0.1	1
153	COARSE BIFURCATION DIAGRAMS VIA MICROSCOPIC SIMULATORS: A STATE-FEEDBACK CONTROL-BASED APPROACH. International Journal of Bifurcation and Chaos in Applied Sciences and Engineering, 2004, 14, 207-220.	1.7	27
154	Atomistic calculation of the SiH3 surface reactivity during plasma deposition of amorphous silicon thin films. Surface Science, 2004, 572, L339-L347.	1.9	26
155	Growth and characterization of hydrogenated amorphous silicon thin films from SiH2 radical precursor: Atomic-scale analysis. Journal of Applied Physics, 2004, 95, 1792-1805.	2.5	21
156	Measurement of absolute radical densities in a plasma using modulated-beam line-of-sight threshold ionization mass spectrometry. Journal of Vacuum Science and Technology A: Vacuum, Surfaces and Films, 2004, 22, 71-81.	2.1	55
157	Mechanism and energetics of dimerization of SiH2 radicals on H-terminated Si()-(2×1) surfaces. Surface Science, 2003, 540, L623-L630.	1.9	6
158	Combined effects of substrate compliance and film compositional grading on strain relaxation in layer-by-layer semiconductor heteroepitaxy: the case of InAs/In0.50Ga0.50As/GaAs(111)A. Surface Science, 2003, 540, 363-378.	1.9	2
159	Absolute densities of N and excited N2 in a N2 plasma. Applied Physics Letters, 2003, 83, 4918-4920.	3.3	70
160	Coarse bifurcation analysis of kinetic Monte Carlo simulations: A lattice-gas model with lateral interactions. Journal of Chemical Physics, 2002, 117, 8229-8240.	3.0	92
161	Abstraction of atomic hydrogen by atomic deuterium from an amorphous hydrogenated silicon surface. Journal of Chemical Physics, 2002, 117, 10805-10816.	3.0	47
162	Atomic-scale analysis of deposition and characterization ofa-Si:H thin films grown from SiH radical precursor. Journal of Applied Physics, 2002, 92, 842-852.	2.5	12

#	Article	IF	CITATIONS
163	"Coarse―stability and bifurcation analysis using stochastic simulators: Kinetic Monte Carlo examples. Journal of Chemical Physics, 2002, 116, 10083-10091.	3.0	113
164	Continuum and atomistic modeling of electromechanically-induced failure of ductile metallic thin films. Computational Materials Science, 2002, 23, 242-249.	3.0	15
165	Strain relaxation and interfacial stability in III–V semiconductor strained-layer heteroepitaxy: atomistic and continuum modeling and comparisons with experiments. Computational Materials Science, 2002, 23, 250-259.	3.0	6
166	Mechanism and activation energy barrier for H abstraction by H(D) from a-Si:H surfaces. Surface Science, 2002, 515, L469-L474.	1.9	27
167	Mechanism of hydrogen-induced crystallization of amorphous silicon. Nature, 2002, 418, 62-65.	27.8	379
168	Modeling of radical-surface interactions in the plasma-enhanced chemical vapor deposition of silicon thin films. Advances in Chemical Engineering, 2001, 28, 251-296.	0.9	36
169	In Situ Probing and Atomistic Simulation of a-Si:H Plasma Deposition. Materials Research Society Symposia Proceedings, 2001, 664, 111.	0.1	17
170	Title is missing!. International Journal of Fracture, 2001, 109, 47-68.	2.2	52
171	Mechanisms and energetics of SiH3 adsorption on the pristine Si(001)-(2×1) surface. Chemical Physics Letters, 2001, 344, 249-255.	2.6	19
172	Molecular dynamics study of the interactions of small thermal and energetic silicon clusters with crystalline and amorphous silicon surfaces. Journal of Vacuum Science & Technology an Official Journal of the American Vacuum Society B, Microelectronics Processing and Phenomena, 2001, 19, 634.	1.6	9
173	Evolution of structure, morphology, and reactivity of hydrogenated amorphous silicon film surfaces grown by molecular-dynamics simulation. Applied Physics Letters, 2001, 78, 2685-2687.	3.3	47
174	Deformation behavior of coherently strained InAs/GaAs(111)A heteroepitaxial systems: Theoretical calculations and experimental measurements. Journal of Applied Physics, 2001, 90, 2689-2698.	2.5	8
175	Multiscale modeling of hard materials: Challenges and opportunities for chemical engineering. AICHE Journal, 2000, 46, 878-882.	3.6	61
176	Mechanism and energetics of dissociative adsorption of SiH3 on the hydrogen-terminated Si(001)-(2×1) surface. Chemical Physics Letters, 2000, 329, 304-310.	2.6	33
177	Interfacial stability and structure in InAs/GaAs(111)A heteroepitaxy: Effects of buffer layer thickness and film compositional grading. Applied Physics Letters, 2000, 77, 3352-3354.	3.3	4
178	Thermal activation of shear modulus instabilities in pressure-inducedbcc→hcptransitions. Physical Review B, 2000, 62, 13799-13802.	3.2	14
179	Mechanical behavior of thin buffer layers in InAs/GaAs(111)A heteroepitaxy. Applied Physics Letters, 2000, 76, 3017-3019.	3.3	11
180	Molecular-dynamics study of the mechanism and kinetics of void growth in ductile metallic thin films. Applied Physics Letters, 2000, 77, 343-345.	3.3	26

#	Article	IF	CITATIONS
181	Current-induced non-linear dynamics of voids in metallic thin films: morphological transition and surface wave propagation. Surface Science, 2000, 461, L550-L556.	1.9	27
182	Effects of buffer layer thickness and film compositional grading on strain relaxation kinetics in InAs/GaAs(111)A heteroepitaxy. Surface Science, 2000, 463, L634-L640.	1.9	4
183	Theoretical study of the energetics, strain fields, and semicoherent interface structures in layer-by-layer semiconductor heteroepitaxy. Journal of Applied Physics, 1999, 85, 3677-3695.	2.5	41
184	Theoretical analysis of electromigration-induced failure of metallic thin films due to transgranular void propagation. Journal of Applied Physics, 1999, 85, 2233-2246.	2.5	105
185	Atomistic simulation study of the interactions of SiH3 radicals with silicon surfaces. Journal of Applied Physics, 1999, 86, 2872-2888.	2.5	63
186	Surface morphology in InAs/GaAs(111)A heteroepitaxy: Experimental measurements and computer simulations. Applied Physics Letters, 1999, 75, 829-831.	3.3	14
187	Theoretical study of the interactions of SiH2 radicals with silicon surfaces. Journal of Applied Physics, 1999, 86, 5497-5508.	2.5	31
188	Nonhydrostatic stress effects on failure of passivated metallic thin films due to void surface electromigration. Surface Science, 1999, 432, L604-L610.	1.9	16
189	Kinetics of strain relaxation through misfit dislocation formation in InAs/GaAs(111)A heteroepitaxy. Surface Science, 1999, 441, L911-L916.	1.9	13
190	Electromigration-induced failure of metallic thin films due to transgranular void propagation. Applied Physics Letters, 1998, 72, 3452-3454.	3.3	59
191	Interfacial stability and misfit dislocation formation in InAs/GaAs(110) heteroepitaxy. Surface Science, 1998, 411, L865-L871.	1.9	16
192	Non-linear analysis of the morphological evolution of void surfaces in metallic thin films under surface electromigration conditions. Surface Science, 1998, 415, L1055-L1060.	1.9	33
193	Abstraction of hydrogen by SiH3 from hydrogen-terminated Si(001)-(2×1) surfaces. Surface Science, 1998, 418, L8-L13.	1.9	62
194	Semicoherent interface formation and structure in InAs/GaAs(111)A heteroepitaxy. Surface Science, 1998, 418, L68-L72.	1.9	26
195	Kinetics of strain relaxation through misfit dislocation formation in the growth of epitaxial films on compliant substrates. Applied Physics Letters, 1998, 73, 753-755.	3.3	25
196	Interactions of SiH radicals with silicon surfaces: An atomic-scale simulation study. Journal of Applied Physics, 1998, 84, 3895-3911.	2.5	60
197	Effects of mechanical stress on electromigration-driven transgranular void dynamics in passivated metallic thin films. Applied Physics Letters, 1998, 73, 3848-3850.	3.3	32
198	Atomistic simulation of SiH interactions with silicon surfaces during deposition from silane containing plasmas. Applied Physics Letters, 1998, 72, 578-580.	3.3	19

#	Article	IF	CITATIONS
199	Atomic-Scale Analysis of Plasma-Enhanced Chemical Vapor Deposition from SiH4/2 Plasmas on Si Substrates. Materials Research Society Symposia Proceedings, 1998, 507, 673.	0.1	1
200	Analysis of Failure in Metallic Thin-Film Interconnects Due to Stress and Electromigration-Induced Void Propagation. Materials Research Society Symposia Proceedings, 1998, 516, 165.	0.1	1
201	Interfacial Stability and Surface Morphology in Layer-By-Layer Semiconductor Heteroepitaxy Luis. Materials Research Society Symposia Proceedings, 1998, 528, 153.	0.1	0
202	Theoretical Analysis of Faceted Void Dynamics in Metallic Thin Films Under Electromigration Conditions. Materials Research Society Symposia Proceedings, 1998, 529, 21.	0.1	2
203	Theoretical Analysis of Electromigration-Induced Failure of Metallic Thin Films. Materials Research Society Symposia Proceedings, 1997, 505, 249.	0.1	1
204	Atomic-Scale Analysis of the Reactivity of Radicals from Silane/Hydrogen Plasmas with Silicon Surfaces. Materials Research Society Symposia Proceedings, 1997, 485, 107.	0.1	2
205	Title is missing!. Journal of Computer-Aided Materials Design, 1997, 4, 63-73.	0.7	19
206	Structure of chemisorbed acetylene on the Si(001)-(2 × 1) surface and the effect of coadsorbed atomic hydrogen. Chemical Physics Letters, 1997, 278, 97-101.	2.6	28
207	Analysis of damage formation and propagation in metallic thin films under the action of thermal stresses and electric fields. Journal of Computer-Aided Materials Design, 1996, 2, 231-258.	0.7	16
208	Theory and Computer Simulation of Grain-Boundary and Void Dynamics in Polycrystalline Conductors. Materials Research Society Symposia Proceedings, 1995, 391, 151.	0.1	8
209	Dynamics of transgranular voids in metallic thin films under electromigration conditions. Applied Physics Letters, 1995, 67, 798-800.	3.3	53